Australian Journal of Basic and Applied Sciences, 5(10): 287-295, 2011
ISSN 1991-8178

Characterization of Nano-Composite Ni Dispersed Over a Silica Matrix Prepared by a Modified Sol-Gel Technique

[1]M.G. Khafag, [2]H.H. Mahmoud, [4]A. Ashiry, [3]M.Q. Israr and [4]I.K. Battisha

[1]Department of Spectroscopy, Physics division, National Research Center, Dokki, Egypt.
[2]Department of radiation Chemistry, National Center for Radiation Research and Technology, Cairo Egypt,
[3]Department of science and technology, Campus Norrköping, Linköping University, SE-60174 Norrköping Sweden.
[4]Department of Solid State, Physics division, National Research Center, Dokki, Egypt.

Abstract: Structural characteristics for silica gel doped with Ni and NiO, prepared by sol-gel method, using tetra-ethoxysilane as precursor material and submitted to different thermal treatment temperature, were investigated through XRD and FTIR, while their morphology through SEM and TEM. The pure silica gel samples heat treated in the range between 60^{o}C up to 700^{o}C have an amorphous phase, while crystalline phase appears at 400^{o}C after annealing of the doped samples in hydrogen gas at 400^{o}C. Measurements of crystallite size of 30 mol % Ni ions dispersed over the amorphous silica matrix sintering at heat treatment temperature 250^{o}C gave rise to a final sample its XRD pattern is characterized by broad Ni peak profiles, corresponding to particle size of 11.8 nm as determined by using the win fit program after reduction in hydrogen at 400^{o}C for 4 hours. Analysis the obtained FTIR spectra, indicates that the sol–gel process used for synthesizing the nano-composites was successful for the entire samples. The hysteresis loops were measured to determine saturation magnetization (Ms), remnant magnetization (Mr) and coercivity (Hc). From these data, it was found that the saturation magnetization for Ni increases, while the coercive field values decrease, by increasing Ni content.

Key words: Sol gel, Hysteresis loop, Ni, Silca gel, nano-composite, FTIR, XRD.

INTRODUCTION

In recent years, there has been an interest in the synthesis and characterization of nanoparticles (Yin *et al*. 2009; Cansella&Aymonier, 2009; Batisha *et al*. 2006). Due to their finite small size, nanoparticles often exhibit novel properties which are different from other materials. Such materials are essential for technological advances in photonics, quantum electronics, sensors and information storage and processing. Nano-composite materials consisting of small metal or metal oxide particles dispersed in glass matrices are attracting much attention because of their potential use in a variety of fields, such as catalysis, optics, magnetism, gas sensing (CO, NO and H_2) applications and electronics. The properties of a nano-composite are strongly dependent on their microstructure with regards to two main features: a) the size distribution of nanoparticles and their dispersion in the host matrix, and b) the interactions that might take place at the nanoparticle/matrix interface. For Me (or MeO)/SiO_2 materials, this kind of interaction can be related to the preparation method (Hotovy *et al*. 2001; Kobayashi *et al* .2003; Heinrichs *et al*. 2008).

Magnetic properties are probably the ones which show the most dramatic dependence on particle size [Coenen1989]. The physical properties of these materials are of interest from both the fundamental and the applied point of view. The dispersion of metallic particles (Co, Cu, Ni, Fe and so on) in matrix gives rise to materials in which the electrical resistivity varies with metal content and a transition from the metallic to the regime is observed when a percolation network is obtained. This transition, which would sharp, actually depends on the dimensions of the metal particles. As a consequence, by varying at the same time volume fraction and particle size the electrical conductivity of the composite can change smoothly by many orders of magnitude (Sun *et al*.2005; Dormer *et al*. 2005).

Up to date, one of the most common and well-studied methods of synthesizing Ni/SiO_2 nano-composites is the sol–gel method. The synthesis of inorganic materials using sol-gel techniques is an attractive field of research worldwide. The sol-gel technique has been proven for several years now to be efficient for the processing of SiO_2 as bulk and thin film materials. The primary attention was paid to the low temperature nature of the sol-gel process. This dictate that, one of the main advantages of the sol-gel process is the low energy cost since silica gel can be obtained at quite low temperature. The sol-gel researchers, however, soon became aware

Corresponding Author: I.K. Battisha, Department of Solid State, Physics division, National Research Center, Dokki, Egypt.
E-mail- szbasha@yahoo.com
Tel- 002-02-25194104, Mob;002/ 0101526515

of the potential of the sol-gel method to provide new advanced functional materials based on the various microstructures (Batisha *et al*. 2009; Batisha *et al*. 2009).

In this paper, we examine whether the sol-gel method is applicable for the preparation of the transition-metal nickel embedded in amorphous silica gel. The prepared samples were submitted to different heat treatment temperatures starting from 60 up to 700°C. Annealed in hydrogen gas at 400°C will be done. The sol–gel based synthesis and characterization of nickel nano-particles in silica glasses by methods of Fourier transform infrared (FTIR), X-ray diffraction (XRD) and transmission electron microscopy (TEM). The saturation magnetization (Ms), remnant magnetization (Mr) and coercivity (Hc), will be determined by measuring the hysteresis loop.

Experimental:

Pure silica gels sintering in the range between 60 and 700°C, were prepared using procedure via the hydrolysis and condensation of $(CH_3CH_2O)_4Si$ tetraethoxysilane TEOS, ethanol and distilled water, in the presence of hydrochloric acid, with molar ratios; 1:6:10:3 for TEOS: CH_3CH_2OH:H_2O:HCl. These solutions filtered, followed by stirring for one hour at room temperature. The resultant homogeneous solutions for preparing bulk materials were filled in moulds and aged in a drying oven type GFL 71.5, at 60◦C for 21 days until no shrinkage appears. The final products were monolithic, clear, transparent, cracks free and cube with dimensions 15×15×3 mm. Densification and crystallization of gel were obtained, by sintering in air for two hr at temperature ranging from 200°C up to 700°C, in a muffle furnace type (Lento) with a heating rate 1.5°C/min. The overall process can be written as:

$$Si(O\text{-}R)_4+4H_2O \rightarrow Si(OH)_4+4C_2H_5OH \quad (R= CH_2CH_3)$$
$$Si(OH)_4 \rightarrow SiO_2+2H_2O$$

Technology of the growth of Ni nano-particles in silica gel glass is clear in Table 1. The nickel was introduced into the system in the form of nitrate esahydrate salt. Because the hygroscopic nature of the salt does not allow its exact weighting, the salt was dissolved in water and the metal content was determined by standard titration. Nickel nitrate was introduced in the initial stage of the process, by dissolving 10 and 30 mol % of nickel nitrate in nitric acid, resulting in a clear green solution then this solution was dissolved in the silica sol-gel solution prepared before. All samples were clear and transparent. The pure samples are transparent and colorless, while the samples containing nickel still transparent clear but have green color. Before the reduction step, gelation, drying and a slow gradual heating in air of the gel was performed followed by thermal treatment at 250°C for 6 hours as shown in Table 1. These treatments were chosen as reasonable compromise between the need for eliminating the solvents and the organic molecules trapped in the gel network and the wish to prevent the massive growth of the thermal oxide nano-particles. Then annealing in the atmosphere of molecular hydrogen at the temperature of 400°C during 4 hr was done, to give us the following compositions ($90SiO_2$:10Ni) and ($70SiO_2$:30Ni).

X-ray diffraction (XRD) patterns from the prepared samples were recorded with a Diano X-ray diffractometer using monochromatized Co $K_{\alpha 1}$ radiation of wavelength λ = 1.79026A˚ from a fixed source operated at 45 kV and 9 mA. Crystallite sizes G were determined from the Scherrer equation (G = k/Dcosh), where 2h is the diffraction for a particular Bragg diffraction peak, and D is the (corrected) full width (in radians) of the peak at half maximum (FWHM) intensity. The correction to the measured FWHM Ds for a sample peak was made to accommodate systemic instrumental broadening and utilized peak widths Dq measured from a diffraction scan, taken under identical conditions, from a strain-free powdered quartz sample, with crystallite size ranging between 5 and 10 lm. The corrected sample peak widths were calculated as $(D_s^2 - Dq^2)^{1/2}$. Micro-strain and crystallite size contributions to D were separated using the Win-Fit program, using standard samples for estimation of instrumental broadening. The final sample crystallite sizes G were obtained by Fourier analysis, using the corrected profile. The diffraction peak used was the most intense diffraction peak, assigned to the (222) reflection, appears at $2\Theta = 52^o$ for 30 % of Ni, respectively**.**

The coarse and fine microstructures of the prepared samples were depicted by transmission and scanning electron microscope (TEM) and (SEM).

The FTIR spectra were collected from the prepared samples using Fourier Transform infrared spectrometer “Jascow FT/IR 430-spectrometer, Japan”. The number of scans was 32 and the resolution was 4 cm^{-1}. All spectra were recorded in the range (4000-400 cm^{-1}). The KBr technique was used to prepare the samples for IR measurements. Magnetic measurements were performed using quantum design magnetometer. The saturation magnetization (Ms), remnant magnetization (Mr) and coercivity (Hc) will be studied by measuring the hysteresis loops.

Table 1: Process of the growth of Ni nano-particles in silica gel glass.

Precursors			
A tetraesoxysilane (TEOS) (Aldrish 98 %)			
B $Ni(NO_3)_2.H_2O$ (Aldrish 98 %)			
C Ethanol (EtOH)			
D Nitric acid			
E Distilled water			
Sol gel preparation			
Starting solution and mixing order (B+ D+ E) in (A+ C)			
Mixing rate: rapid			
Stirring time: 60 min			
Temperature during stirring: RT			
TEOS/ EtOH/Water molar ratio: 0.028: 0.174: 0.28			
Gelation			
Temperature: RT		Aging: 2 Days at RT	
Drying			
Ramp	T_{max}	Dwell time (T_{max})	
5°/ day	90°C	1 day	
Mechanical treatment			
Grinding in a gate mortar			
Heat treatments in air			
Ramp	T_{max}	Dwell time (T_{max})	
10°/ min	250°C	6 hours	
Reduction treatments (H_2)			
Ramp	T_{max}	Dwell time (T_{max})	Flow
10°/ min	400°C	4 hours	45 ml/min

The magnetic properties of the prepared sample were measured at room temperature in a vibrating sample magnetometer under a maximum applied field of about 10 kO_e.

Results:

XRD patterns of bulk silica gel samples dried at 60◦C for 3 weeks and heat treated for 2 hr at temperature ranging from 200 up to 700◦C are shown in Fig. 1.

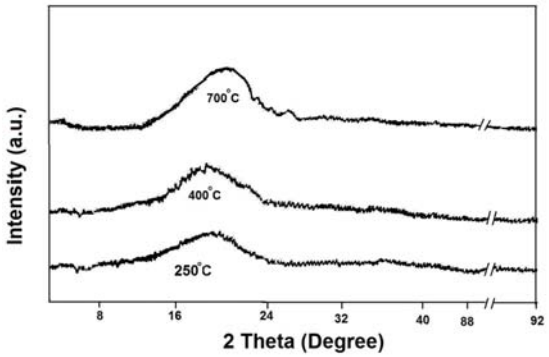

Fig: 1: XRD patterns of monolith pure silica gel, sintering at 3 different heat treatment temperature 250, 400 and 700°C.

Fig 2 shows the XRD patterns of monolith silica gel doped with 30 mol % of nickel nitrate ($70SiO_2$:30Ni), sintering at 250°C and then reduced by hydrogen for 4 hours at 400°C after sintering at heat treatment temperature 250°C. In Fig 2. the Ni species appeared at 2 □ = 52 and 61.9 ° together with a small hump at 2 □ = between 20 and 30°.

In order to confirm the formation of silica matrix as well as Nickel and nickel oxide, the samples were analyzed by FTIR. Figure 3 (a-d) exhibits the FTIR spectra for silica gel doped with 10 mol % of NiO, ($90SiO_2$:10NiO) sintered at heat treatment temperature 60, 100, 400 and 700°C, respectively.

The FTIR spectrum shown in Figure 4 highlight the structural evolution of $90SiO_2$10Ni sintered at heat treatment temperature 250 °C and then reduced at 400°C in hydrogen gas for 4 hours.

The electron microscope TEM micrograph of (a) $90SiO_2$10Ni and (c) $70SiO_2$ 30Ni, and their representative TEM selected area electron diffraction (SAED) patterns (b) and (d) for Ni nano-particles dispersed in silica gel glass and reduced in hydrogen gas at 400°C was performed to determine their size and shape as shown in Fig. 5 (a - d).

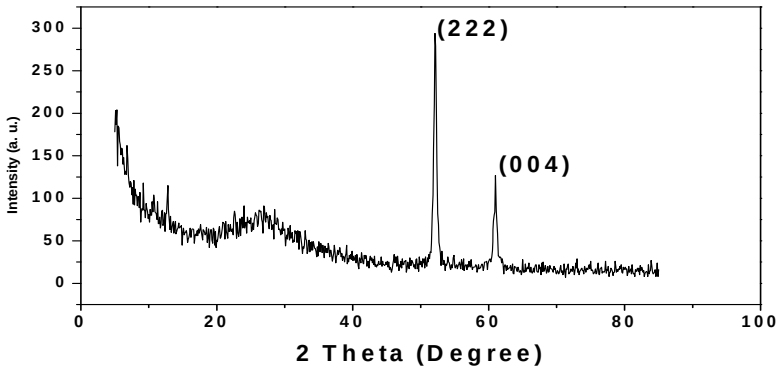

Fig. 2: XRD patterns of monolith $70SiO_2$:30Ni, sintered at heat treatment temperature 250°C and then annealed at 400°C in hydrogen gas for 4 hours.

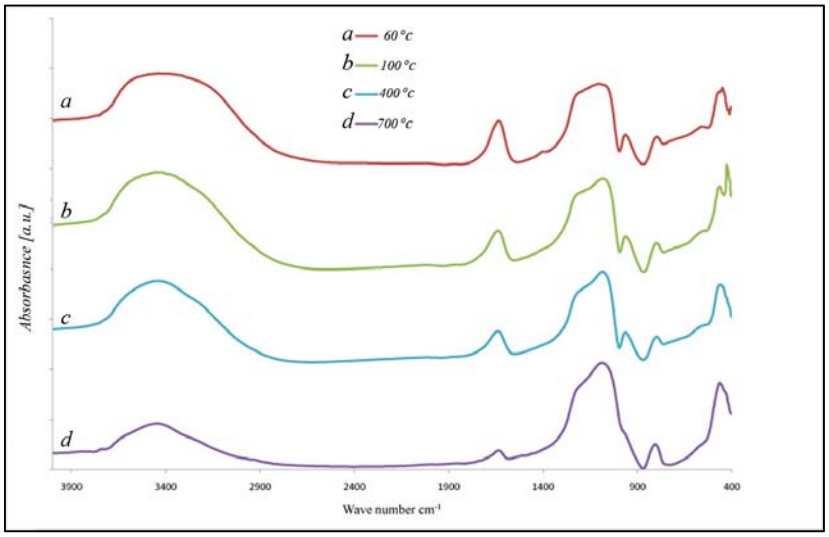

Fig. 3: FTIR spectra of $90SiO_2$10NiO, heated at different sintering temperature (a) 60, (b) 100, (c) 400 and (d) 700°C.

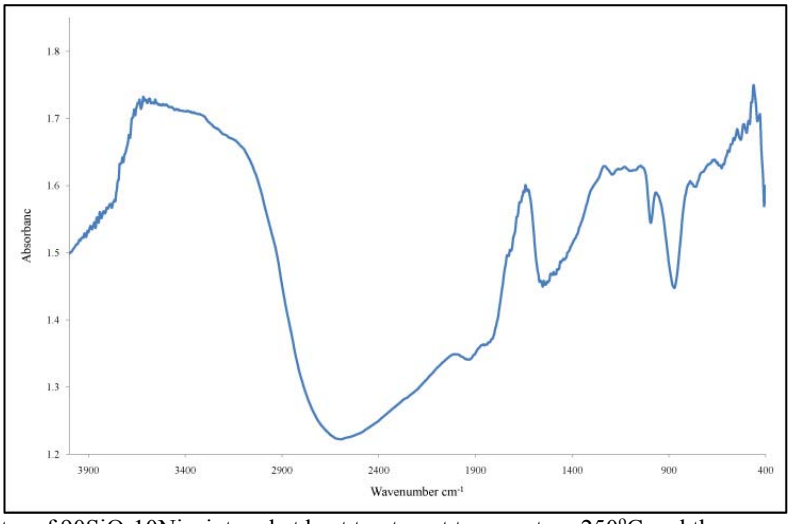

Fig. 4: FTIR spectra of $90SiO_2$10Ni, sintered at heat treatment temperature 250°C and then annealed at 400°C in hydrogen gas for 4 hours.

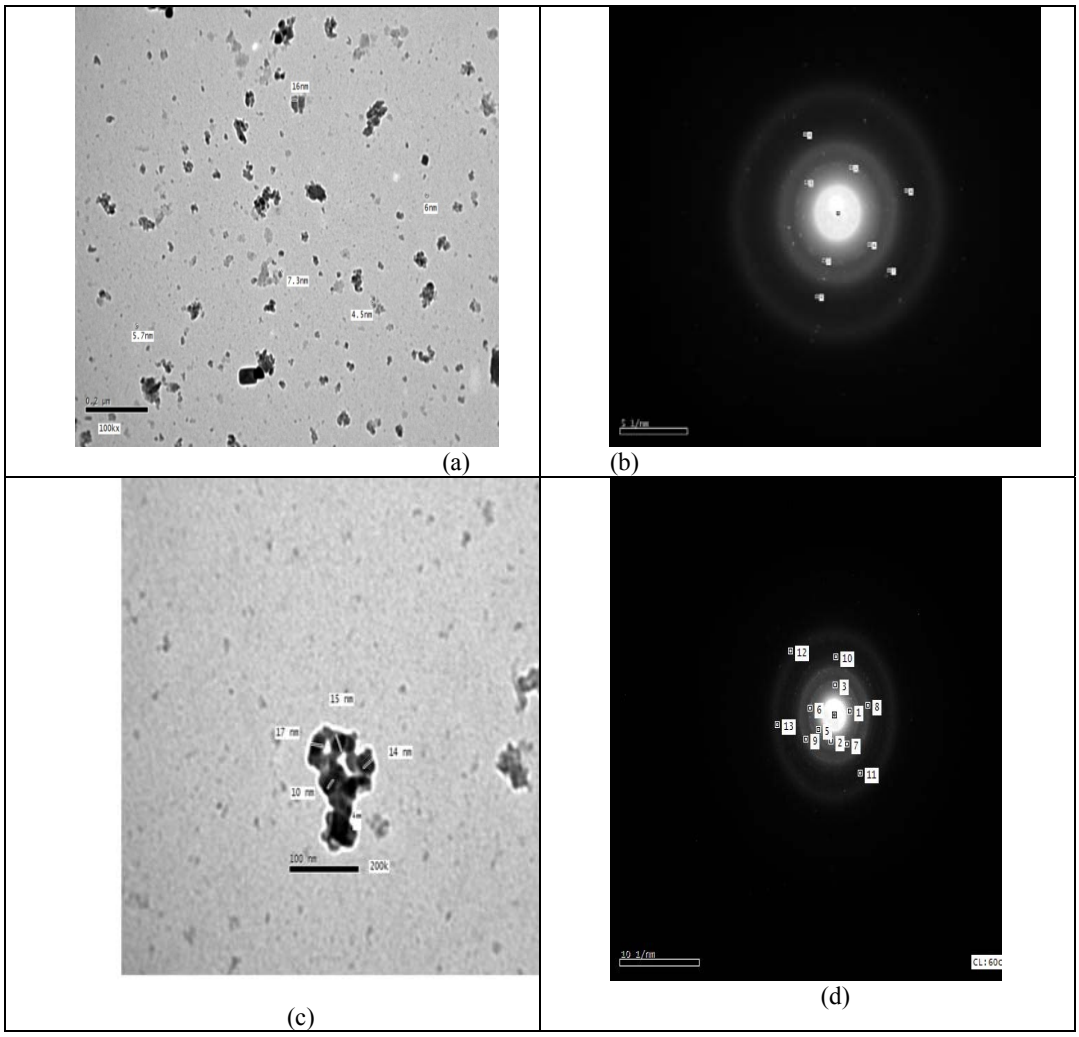

Fig. 5: Transmission electron microscope (TEM) of (a) $90SiO_2$10Ni and (c) $70SiO_2$30Ni in the form of monolith, and their TEM diffraction pattern (b) and (d), heat treatment temperature 250^{o}C and then annealed at 400^{o}C in hydrogen gas for 4 hours.

Fig. 6 shows SEM images of $90SiO_2$:10Ni and $70SiO_2$30Ni nano-particles monolithic samples thermally synthesized at 250^{o}C for one hour and then reduced in hydrogen at 400^{o}C for 4 hours.

Fig 7. Shows typical EDX spectrum of silica gel doped with 30 mol % Ni in the form of monolith, heat treatment temperature 250^{o}C and then annealed at 400^{o}C in hydrogen gas for 4 hours.

Fig. 8 shows the magnetic hysteresis loops of $70SiO_2$30Ni and $90SiO_2$10Ni nano-composites. The hysteresis loops were measured to determine parameters such as the saturation magnetization (Ms), remnant magnetization (Mr) and coercivity (Hc).

Discussion:

XRD patterns of bulk silica gel samples dried at 60◦C for 3 weeks and heat treated for 2 hr at temperature ranging from 200 up to 700◦C are shown in Fig. 1. No peaks are observed for samples fired up to 700◦C except the hump at 2θ between 12 and 24◦, which is attributed to amorphous silica. These results are in good agreement with the previously published by the sharing of one of the authors [Batisha *et al*.2002].

Fig 2 shows the XRD patterns of monolith silica gel doped with 30 mol % of nickel nitrate ($70SiO_2$:30Ni), sintering at 250^{o}C and then reduced by hydrogen for 4 hours at 400^{o}C after sintering at heat treatment temperature 250^{o}C. In Fig 2. the Ni species appear at 2 □ = 52 and 61.9 ^{o} together with a small hump at 2 □ = between 20 and 30^o. Crystalline phase of Ni_2SiO_4 is appearing due to the presence of Ni dispersed on the amorphous silica gel. The most intense diffraction peak, assigned to the (222) reflection from the nickel transition element, appears at 2 □ = 52^o, along with less intense peaks from it assigned to the (004) at 2 □ = 61.9^o (by reference to JCPDS files 03 -0780) (Takahashi *et al*. 2003; Takahashi *et al.,* 2005). The crystalline

phase which appears in Fig 2 is not observed in the diffraction of pure silica sample sintered at the same heat treatment temperature. The crystallite size calculated from the broadening of the most intense diffraction peak, using the Win Fit program, appears at 2 □ = 52 ^{o} for 10 mol % of Ni, were found to be equal to about 11.8 nm.

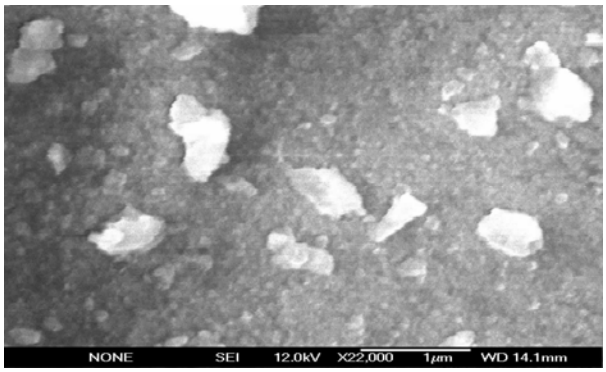

(a)

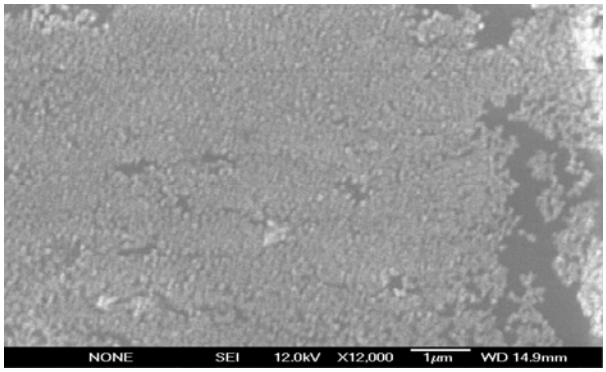

(b)

Fig. 6: The SEM micrograph of a) $90SiO_2 10Ni$ and (b) $70SiO_2 30Ni$ samples sintering at heat- treatment temperature 250^{o}C for one hour and then reduced in hydrogen at 400^{o}C for 4 hours.

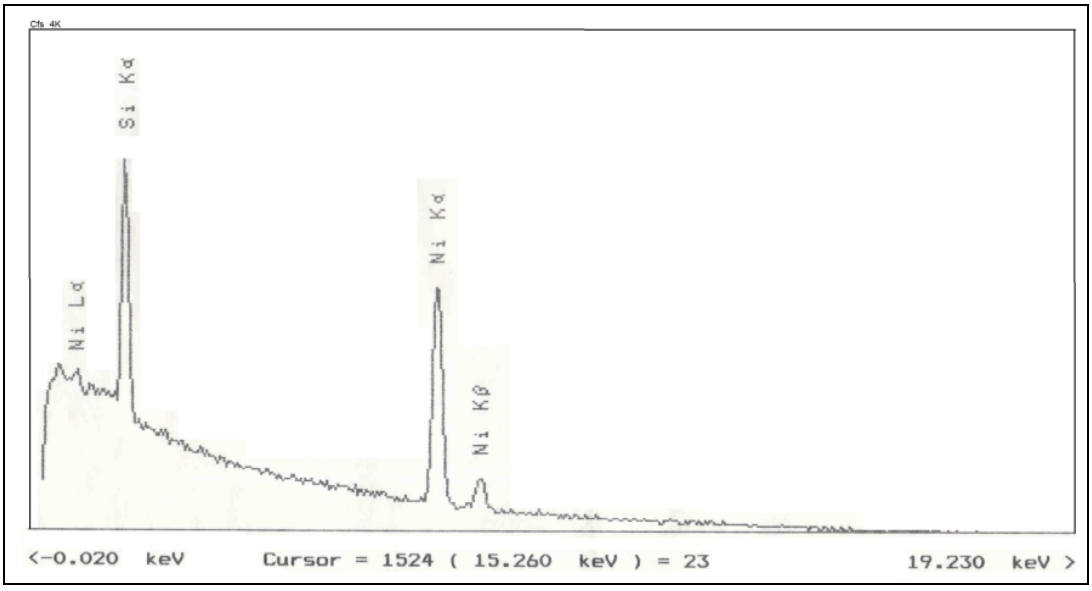

Fig. 7: Typical EDX spectrum of $70SiO_2 30Ni$, sintered at heat treatment temperature 250^{o}C and then annealed at 400^{o}C in hydrogen gas for 4 hours.

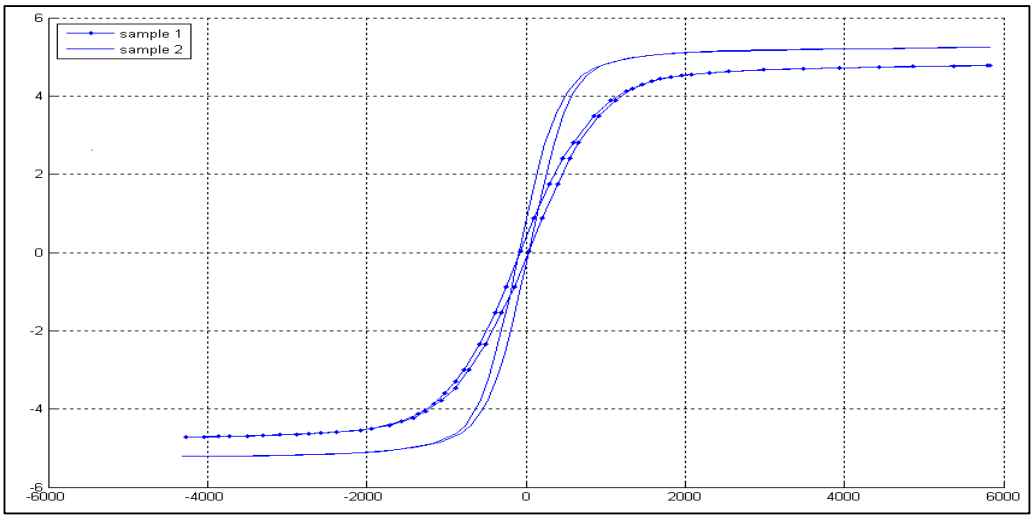

Fig. 8: The magnetic hysteresis loops of $90SiO_2$10Ni (sample1) and $70SiO_2$30Ni (sample 2) nano-composite, sintered at heat treatment temperature 250°C and then annealed at 400°C in hydrogen gas for 4 hours

Figure 3 (a-d) exhibits the FTIR spectra for silica gel doped with 10 mol % of NiO, ($90SiO_2$:10NiO) sintered at heat treatment temperature 60, 100, 400 and 700°C, respectively. In all the spectra, the broad band between 3800 and 2800 cm^{-1} is mainly related to the overlap of O–H vibration modes in residual silanol groups (Si–OH) that remain in the matrix and did not complete the condensation process and to chemisorbed water molecules. The signal at around 1635 cm^{-1} is assigned to the υ (O H) stretching vibration of different Si- OH groups, due the strong hydrogen bond of intermolecular. It is due to the deformation modes of δ (H–O–H) and attributed to bending vibration of crystalline water, which could come from KBr in the pellets and adsorbed water (Wu *et al*.2006;Takeuchi *et al*. 2007). It is slightly shifted to higher wavenumber by increasing the heat treatment temperature up to 700°C. The presence of these absorption bands suggests that some of OEt groups were hydrolyzed to hydroxyl (OH) groups and poly-condensed.

The main contribution of the two species 962 cm^{-1} and at 1635 cm^{-1} to the entire band is demonstrated by monitoring its intensity, each associated to O–H stretching vibrations in Si–OH groups [Wu *et al*.2007, Li *et al*.2000] and H_2O molecules, respectively. The intensity of these bands is observed to decreased gradually by increasing the sintering heat treatment temperature, while the band at 962 cm^{-1} completely disappeared at temperature 700◦C indicating full silica poly-condensation process. This is also confirmed by the growing of the 799 cm^{-1} band which is attributed to the formation of Si-O-Si.

There is observed a broad shoulder at 1200 cm^{-1}, which was assigned to stretching vibration of Si–O–Si bonds; this shoulder may be associated also with a combination of vibrations of the nitrate and the CH species [30]. The most intense band in the 1070–1100 cm^{-1} range is demonstrating the Si–O–Si anti-symmetric stretch vibration, this peak position shifts towards lower wave-number with increasing temperature. The NiO gives a band around 455 cm^{-1} at increasing temperature. This band is overlapping with the bending Si-O band at 445 cm^{-1}, as pointed out by Almeida *et al*., [31,32]. When the Ni-Si complex gel powder was heated to 700°C, NiO segregated from silica matrix. This was confirmed by the broadening of the IR absorption bands due to Si-O asymmetric stretching vibration and the increase in the relative intensity of the FTIR band due to Si-O-Si bending vibration, similar to that reported in the literature (Casu *et al*. 2001,;Benjaram *et al*. 2006).

The FTIR spectrum shown in Figure 4 highlights the structural evolution of $90SiO_2$10Ni sintered at heat treatment temperature 250 °C and then reduced at 400°C in hydrogen gas for 4 hours. Strong bands associated with OH stretching vibrations of water and hydroxyl groups occur between 3200 and 3700 cm^{-1}. Water of hydration can be easily distinguished from hydroxyl groups by the presence of the H–O–H bending motion, which produces a medium band at 1637 cm^{-1}. Free water has a strong broad absorption band centered in the region 3200–3400 cm^{-1}. The main band in the 1070–1100 cm^{-1} range which is assigned to Si–O–Si anti-symmetric stretch vibration, shifts toward lower wave number compared to the heat-treated samples showed in Fig. 3. A new band is observed to appear at 1114 cm^{-1} due to the vibrational stretches of Si-O bonds of bulk SiO_2, while the shoulder at 1200 cm^{-1} for the non-reduced samples shifts toward higher wave-number at 1226 cm^{-1} after reduction in hydrogen. The broad bands in the range 1226 - 960 cm^{-1} and broadband at 790 cm^{-1} may be due to stretching mode of broken Si-O- bridges. The two bands assigned to Si-OH and Si-O-Si appeared at 966 and 796 cm^{-1}, for samples doped with NiO shifted to 960 and 790 cm^{-1} for reduced sample doped with Ni which argue the presence of Si–O-Ni bonds. New absorption bands are observed to appear at 669 and 526 cm^{-1}.

The bands between 500 and 750 cm^{-1} in FTIR seems to confirm the presence of metal hydroxide stretching (Smith1999; Parven *et al*. 2009).

Based on the FT-IR data, the following conclusion could be deduced: NiO nanoparticles, formed in cavities of the amorphous silica matrix, act as an obstacle towards the spontaneous silica poly-condensation process.

After annealing at 400°C under H_2 atmosphere, to induce the nucleation of metallic Ni precipitates, another system is formed displaying a much better crystalline order. This result is confirmed by SEM. No O atoms are detected in the first shell around Ni. Hence a first assumption that considers H being trapped in the samples and reacting with the Ni, Si and O atoms

This FTIR study of the surface phenomena has confirmed the advantages of the FT-IR spectroscopy as an investigation structural method in regards to the nano-surface phenomena and surface atom groups.

The electron microscope TEM micrograph of (a) $90SiO_2$10Ni and (c) $70SiO_2$ 30Ni, and their representative TEM selected area electron diffraction (SAED) patterns (b) and (d) for Ni nano-particles dispersed in silica gel glass and reduced in hydrogen gas at 400°C was performed to determine their size and shape as shown in Fig. 5 (a - d). TEM micrographs for a reduced sample (a) $90SiO_2$10Ni show many dark spheres which are individual Ni nano-particles. It is assured that Ni particles distribute homogeneously in the silica matrix. The particle size of 10 mol % Ni in the TEM micrographs was equal to 7.9 nm.

TEM micrographs of $70SiO_2$30Ni, Fig 5 (c) show the presence of very small nickel with higher particle sizes = 12 nm homogeneously distributed in the silica matrix and well agrees with that estimated from the XRD peak broadening 11.8 nm. The obtained patterns are typical of nano-crystalline SiO_2 doped with Ni. The images prove the creation of the nearly spherical Ni nano-particles (Tomiyama *et al*., 2002).

Fig. 6 shows SEM images of $90SiO_2$:10Ni and $70SiO_2$30Ni nano-particles monolithic samples thermally synthesized at 250°C for one hour and then reduced in hydrogen at 400°C for 4 hours. These images clearly show that many of the particles are nearly spherical with very fine crystallite size and highly dispersed without large aggregates especially in the higher content one, but at 10 mol %, it is with some aggregates and accumulations in it. It can be seen that increasing the Ni content is effective to increase the density and improve the microstructure homogeneity of the prepared monolithic samples. Then one can conclude that the particles are less agglomerated at higher Ni content and the particle distribution is more-uniform.

From all above results, it is clear that silica gel doped with two different concentrations of Ni stoichiometric are crystallized directly by preparing it by sol gel technique.

Fig 7. shows typical EDX spectrum of silica gel doped with 30 mol % Ni in the form of monolith, heat treatment temperature 250°C and then annealed at 400°C in hydrogen gas for 4 hours, whereby the Si, O and Ni contributions can be clearly seen. EDX analysis reveals a Ni loading weight atomic % with respect to Si and O as shown in Table 2.

Table 2: Typical EDX (weight and atomic %) of $70SiO_2$30Ni in the form of monolith, heat treatment temperature 250°C and then annealed at 400°C in hydrogen gas for 4 hours.

Atomic %	Weight %	Line	Element
81.15	67.32	K	Si
18.85	32.68	L	Ni

Table 3: Magnetic parameters of monolith $70SiO_2$30Ni (sample 1), $90SiO_2$10Ni (sample 2), sintered at heat treatment temperature 250°C and then annealed at 400°C in hydrogen gas for 4 hours.

Hc G	Mr emu/g	Ms emu/g	Crystallite size (nm)	Sample
65.66	.4311	4.781	6 nm	$90SiO_2$10Ni sample (1)
61.99	1.622	5.253	12 nm	$70SiO_2$30Ni Sample (2)

Magnetization, (B) (emu/g):

The magnetic behavior of $70SiO_2$30Ni, $90SiO_2$10Ni nano-composites is dictated by the magnetic properties of the composites influenced by mean crystallite sizes. Thus owing to higher values of crystallite size of silica gel doped with 30 mol % of Ni compared with the sample doped with 10 mol % of Ni , in the former case the hysteresis loops are less closed, while for the other one hysteresis loops are more closed. According to the literature, when nano-particles are included in silica matrix, their magnetic anisotropy exhibits a pronounced increasing (Caizer& Hrianca, 2003). Fig. 8 shows the magnetic hysteresis loops of $70SiO_2$30Ni and $90SiO_2$10Ni nano-composites. The hysteresis loops were measured to determine parameters such as the saturation magnetization (Ms), remnant magnetization (Mr) and coercivity (Hc), as shown in Table 3. As it can be seen, the magnetic properties of the samples clearly depend on the nickel loading and the nickel particle size. It is evident from Fig. 8 that the saturation magnetization (Ms) decreases with decreasing Ni content, as expected, since this parameter depends on the total mass of the magnetic material. The reduction of this value may be caused by non-colinearity of the magnetic moments at the surface of the nano-particles, resulting in a decrease

of the saturation magnetization for a lower Ni content (Ma *et al*., 2003). The decrease in remnant magnetization (Mr) can be attributed to a decrease of the mean size of nano-crystallites. On the other hand, the super-Para magnetism is often observed for magnetic particles below 10 nm (Li *et al*. 2000). One can see that the values of the saturation magnetization for Ni increase, while the coercive field values decrease, by increasing Ni content.

Conclusion:

Modified sol-gel technique was successfully used for preparing pure silica gel (SiO_2) and nano-composite SiO_2: NiO and submitted to different heat treatment temperature starting from 60 up to 700°C. The XRD diffraction patterns revealed that the crystalline phase appeared in the doped samples was not appeared in the pure silica sample sintered at the same heat treatment temperature and reduced in hydrogen at 400 C for 4 hours. The crystallite size calculated from the broadening of the most intense diffraction peak, appears at 2 □ = 52° for the doped sample with 30 mol % of Ni, were found to be equal to about 11.8 nm. The obtained result from XRD was confirmed by TEM and give 12 nm as crystallite4 size. After analyzed the obtained FTIR spectra, the results indicate that NiO nano-particles, formed in cavities of the amorphous silica matrix, act as an obstacle towards the spontaneous silica polycondensed process, which indicate that the sol–gel process used for synthesizing the nanocomposites is successful for the entire samples.

Effects of the nickel content on the magnetic properties of $90SiO_2$10Ni and $70SiO_2$30Ni nano-composites have been studied, the saturation magnetization (Ms), remnant magnetization (Mr), decreased with decreasing Ni content. The magnetic properties have shown the increase of the Ms and Mr and the decrease in Hc of the samples with increasing Ni contents.

REFERENCES

Almeida, R.M., C.G. Pantano, 1990. J. Appl. Phys., 68: 4225. Battisha I.K., Afify H.H., Badr Y., J. Sol-Gel Science and Technology, 25: 5.

Battisha, I.K., H.H. Afify M. Ibrahim, 2006. J. Magnetism and Magnetic Materials, 306(2): 211.

Battisha, I.K., Y. Badr, N.M. Shash, M.G. El-Shaarawy, A.G.A. Darwish, 2009. J. Sol-Gel Sci Technol DOI 10.1007/s, 10971: 2129-5.

Battisha, I.K., M.A. Salem, A.M.S. Nahrawy, Y. Badr, B. Elouady, M. Kamal, 2009. Int. J. Nano and Biomaterials, 2 Nos. 1/2/3/4/5.

Benjaram M. Reddya, Gundapaneni M. Kumara, Ibram Ganesh, Ataullah Khana, 2003. J. Molecular Catalysis A: Chemical 247, 80 (2006).Caizer C., Hrianca I., Eur. Phys. J., B31: 391.

Cansella, F., C. Aymonier, 2009. J. Supercritical Fluids, 47: 508.

Canut, B., M.G. Blanchin, V. Teodorescu, A. Traverse, 2007. J. Non-Cryst. Solids, 353: 2646.

Casu, M., A. Lai, A. Musinu, G. Piccaluga, S. Solinas, 1989. J. Mate. Scien., 36: 3731.

Coenen, J.W.E., 1989. Appl. Catalysis, 54: 65.

Devit, N.T.Mc., W.L. Baun, 1964. J. Spectrochimica Acta, 20: 799.

Dormer, K., Seeney Ch., K. Lewelling, G. Lian, D. Gibson, M. Johnson, 2005. Biomaterials, 26: 2061.

Heinrichs, B., L. Rebbouh, J.W. Geus, S. Lambert, H.C.L. Abbenhuis, F. Grandjean, G.J. Long, J.P. Pirard, R.A. Santen, 2008. J. Non-Cryst. Solids, 354: 665.

Hotovy, I., J. Huran, P. Siciliano, S. Capone, L. Spiess, V. Rehacek, 2001. J. Sensors and Actuators, B78: 126.

Kobayashi, T., M. Haruta, M. Ando, 2003. J. Sensor and actuators, B 13-14: 545.

Lenzi, G.G., M.K. Lenzi, M.L. Baesso, A.C. Bento, L.M.M. Jorge, O.A.A. Santos, 2008. J. Non-Cryst. Solids, 354: 4811.

Li, L., G. Li, R.L. Jr. Smith, H. Inomata, 2000. J.Chem. Mater. 12, 3705 (2000).Li L., Li G., Smith R.L., Inomata H., J.Chem. Mater, 12: 3705.

Ma, M., Y. Zhang, X. Li, D. Fu, H. Zhang, N. Gu, 2003. J. Colloid Surf., A 224: 207.

Parveen, M.F., S. Umapathy, V. Dhanalakshmi, R. Anbarasan, 2009. J. Materials Science, 44(21). Smith B., Inorganic compounds, pp: 168-71, CRC Press, Boca Raton, F.L., 1999.

Sun, Y., L. Duan, Z. Guo, Y. DuanMu, M. Ma, L. Xu, Y. Zhang, N. Gu, 2005. J. Magn. Magn. Mater, 285: 65.

Takahashi, R., S. Sato, T. Sodesawa, M. Suzuki, N. Ichikuni, 2003. J. Microporous and Mesoporous Materials, 66: 197.

Takahashi, R., S. Sato, T. Sodesawa, S. Tomiyama, 2005. J. Applied Catalysis A: General, 286: 142.